Experimental Study of Enhanced Active Resonant DC Circuit Breakers

Tim Augustin, Marley Becerra, *Senior Member, IEEE*, and Hans-Peter Nee, *Fellow, IEEE*

***Abstract*—Enhanced active resonant (EAR) dc circuit breakers (DCCBs) are a novel type of DCCB that use a discharge closing switch as interruption medium. A technical limitation of discharge closing switches is the minimum voltage across the main gap required for successful triggering. A novel commutation process creating the minimum voltage internally is proposed, which allows to simplify the EAR DCCB configuration and to reduce its component count. In the prototype, the discharge closing switch is implemented with a TVG. Experiments show that the TVG can be triggered reliably down to a voltage of 50 V and that the discharge in the TVG is highly oscillatory at low current. The originally proposed EAR DCCB configuration has to be tuned such that the commutation to the TVG succeeds at low current. Conversely, the novel commutation process decouples the minimum voltage from the current level by adjusting the triggering delay. This allows reliable commutation irrespective of the operating conditions. It is shown that the novel commutation process does not adversely affect dc interruption. Proactive commutation operation and auto-reclosing strategies are demonstrated.**

***Index Terms*—DC circuit breakers (DCCBs), dc power systems, gas discharge devices, HVdc circuit breakers, spark gaps.**

I. Introduction

POWER electronics-dominated dc grids are evolving around the world to integrate intermittent renewable energy sources. Such dc grids will play an important role in the power system of the future. The dc faults, however, pose a threat to dc grids since the fault currents rise rapidly and many commonly used voltage-source converters cannot control the dc-side current during the fault. Hence, dc circuit breakers (DCCBs) are crucial components needed to handle dc faults in power electronics-dominated dc grids [1].

Various DCCB topologies have been proposed and an overview of DCCBs is given in [2]. Most DCCBs are either current-injection DCCBs or hybrid DCCBs. Current-injection DCCBs use an arcing mechanical switch as interruption medium with an injection circuit that injects a counter current into the arcing mechanical switch to force a local current zero crossing [3]–[10]. This extinguishes the arc and interrupts the dc. Hybrid DCCBs use power semiconductors as interruption medium and commutate the DCCB current from normally conducting mechanical switches to power semiconductors that interrupt the dc [11]–[20]. Hybrid DCCBs have substantially lower ON-state losses than solid-state DCCBs. On the one hand, power semiconductors with turn-OFF capability are expensive. On the other hand, power semiconductors with turn-OFF capability increase the flexibility of hybrid DCCBs and, depending on the concept, allow advanced functionality, such as *proactive commutation* and *fault current limitation*. Proactive commutation compensates for protection delay [21] and provides fast backup protection. Fault current limitation increases interruption speed and reduces the peak energy [22] as well as the stress on the converters.

The tube-based DCCBs described in [23] and [24] operate similarly to hybrid DCCBs. The tubes used must be able to turn ON and OFF similar to power semiconductors with turn-OFF capability. The hybrid DCCBs in [25]–[27] use thyristors instead of power semiconductors with turn-OFF capability. The thyristors must be turned OFF with an external circuit comparable to an injection circuit. The enhanced active resonant (EAR) DCCBs introduced in [28] are tube-based DCCBs that use discharge closing switches (DCSs) as interruption medium. DCSs are like discharge-based thyristors because DCSs can be turned ON and not OFF. Thus, EAR DCCBs depend on an injection circuit for turn-OFF similar to current-injection DCCBs and thyristor-based hybrid DCCBs. Nonetheless, EAR DCCBs internally operate similarly to hybrid DCCBs, thus offering comparable functionality. In addition, EAR DCCBs allow for a design with an asymmetric interruption capability. This implies that the EAR DCCB works as an hybrid DCCB in one current direction and as a current-injection DCCB in the other current direction.

The knowledge about EAR DCCBs and their properties is still limited. The operation modes of originally proposed EAR DCCBs were explained in [28]. However, the preliminary test results only demonstrated the basic operating principle of EAR DCCBs. Augustin *et al.* [29] focused exclusively on the actuator of the mechanical switch used in EAR DCCBs. The main contribution of this article is an indepth experimental study of the EAR DCCBs in various operating modes and of a novel commutation process. As explained in [28], operating scenarios, such as load current interruption and high impedance faults, with relatively low current can be challenging for EAR DCCBs, because of the minimum voltage requirement of the DCS. The article also

Manuscript received July 9, 2021; revised October 17, 2021; accepted November 30, 2021. Date of publication December 7, 2021; date of current version January 19, 2022. The work of Tim Augustin was supported through SweGRIDS, in part by the Swedish Energy Agency and in part by Hitachi ABB Power Grids. The work of Marley Becerra was supported by the Swedish strategic research program StandUp for Energy. Recommended for publication by Associate Editor E. Babaei. *(Corresponding author: Tim Augustin.)*

The authors are with the KTH Royal Institute of Technology, Teknikringen 33, 10044 Stockholm, Sweden (e-mail: timau@kth.se; marley@kth.se; hansi@kth.se).

Color versions of one or more figures in this article are available at https://doi.org/10.1109/TPEL.2021.3133386.

Digital Object Identifier 10.1109/TPEL.2021.3133386

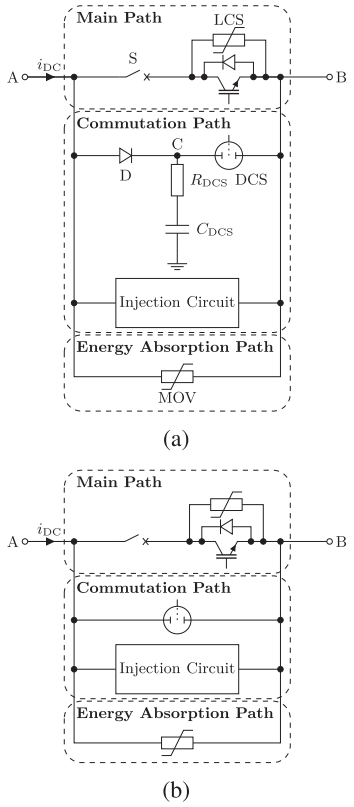

Fig. 1. Unidirectional EAR DCCBs. (a) Originally proposed configuration. (b) Simplified configuration.

addresses this open question by experimentally studying the characteristics of the DCS and the commutation processes at low current and low voltage. The novel commutation process proposed in this article allows to simplify EAR DCCBs and to reduce the component count by a resistor, capacitor, and diode valve rated for DCCB voltage, respectively. The novel commutation process also improves the performance and reliability of EAR DCCBs by generating a voltage sufficiently above the minimum voltage irrespective of the current level.

The rest of this article is organized as follows. Section II describes EAR DCCBs and the novel commutation process. Section III explains the prototype, the test circuit, and the test procedures. Section IV studies the triggering of the DCS, the commutation processes, dc interruption after the novel commutation process, proactive commutation, and auto-reclosing strategies in experiments. Section V discusses the experimental results and their impact on the design of EAR DCCBs. Finally, Section VI concludes this article.

II. EAR DCCBs

A. Overview

The EAR DCCBs were introduced in [28]. The originally proposed unidirectional EAR DCCB configuration is shown in Fig. 1(a). The core of all EAR DCCBs is a DCS in the commutation path that replaces the power semiconductors with turn-OFF capability used in hybrid DCCBs. The main path is implemented with a mechanical switch S and a load commutation switch

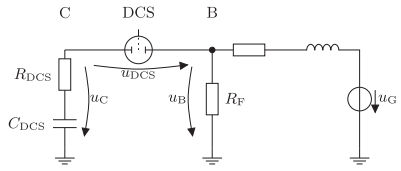

Fig. 2. Equivalent circuit of the originally proposed EAR circuit breaker configuration during the triggering of the discharge closing switch.

(LCS) similar to [11]. DCSs are discharge-based devices that only turn OFF at current close to zero comparable to thyristors. An injection circuit as used in current-injection DCCBs is applied to force a current zero crossing in the DCS for turn-OFF and to interrupt the dc i_{DC}. The operation states of the originally proposed EAR DCCB configuration were explained in [28] for several operating scenarios. The use of DCSs is beneficial in terms of costs, reliability, robustness, current and voltage ratings, and footprint.

Bidirectional EAR DCCB configurations were described in [28] as well. EAR DCCBs allow to implement bidirectional configurations with symmetric or asymmetric interruption capability. Asymmetric bidirectional EAR DCCB configurations imply that the interruption time or the functionality provided is not same in both current directions. Despite the similarities with current-injection DCCBs, EAR DCCBs offer functionality comparable to hybrid DCCBs, for instance proactive commutation. Auto-reclosing operation in overhead line systems can be executed either by turning ON the main path or by first turning ON the commutation path, and then, commutating i_{DC} to the main path.

B. Minimum Voltage Requirement

The voltage between the anode C and cathode B of the DCS u_{DCS} has to exceed a minimum voltage to turn ON when triggered. The minimum voltage depends on the particular DCS technology and is a limiting factor for the operation of EAR DCCBs. The voltage potentials at the anode u_C and cathode u_B determine the voltage across the DCS $u_{DCS} = u_C - u_B$, as shown in Fig. 2. The RC circuit in the commutation path is charged from the dc line through the diode D to provide the voltage potential u_C with approximately the same magnitude as the dc bus voltage u_G.

The voltage potential at the cathode u_B is approximately equal to u_G. When a dc-side fault occurs toward terminal B of the DCCB, u_B decreases below u_G. However, the decrease of u_B depends on the fault resistance R_F. Severe fault currents flow during solid faults with $R_F = 0$, the dc line voltage collapses and, hence, $u_B = 0$. Consequently, $u_{DCS} = u_C - 0 = u_C$ and the voltage across the DCS approximately equals u_G, which exceeds the minimum voltage substantially. If, however, R_F is high or for load current interruption ($R_F = \infty$), u_B is equal to or slightly different from u_G. In this case, u_{DCS} would be small and almost zero. If u_{DCS} is lower than the minimum voltage of the DCS, the DCS can mistrigger and the EAR DCCB cannot commutate properly. Even though high resistance faults and load current are not critical for the dc system, because of the low

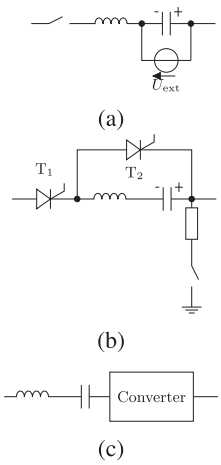

Fig. 3. Main types of injection circuit topologies. (a) Pre-charging from external power supply [6]. (b) Pre-charging from dc line [4]. (c) Successive oscillation technique [7].

current level and redundancy in various EAR DCCB topologies to handle mistriggering [28], the limitations due to the minimum voltage still have to be quantified experimentally. Moreover, the stability of the discharge in the DCS at low current must be investigated.

C. Injection Circuit

Injection circuit topologies can be grouped into three characteristic types with examples shown in Fig. 3: precharged with an external power supply [see Fig. 3(a)], precharged from the dc line [see Fig. 3(b)], and injection current build-up with successive oscillations [see Fig. 3(c)]. If an external power supply is used to precharge the injection circuit as in Fig. 3(a), the external power supply has to be rated for a voltage in the order of magnitude of the dc line voltage. The switch is closed to discharge the precharged capacitor such that the injection current causes a current zero crossing. Injection circuits that are precharged from the dc line require more switches than injection circuits with external power supply, for instance two thyristors T_1 and T_2 in the topology from [4], as shown in Fig. 3(b). Before operating, the grounding switch is closed to provide a charging path to ground and T_1 is fired to start charging from the dc line. When the injection circuit is activated, T_2 is fired causing an oscillation in the LC circuit that reverses the polarity of the capacitor. T_1 is fired again to discharge the capacitor such that the injection circuit causes a current zero crossing. In the successive oscillation technique [7] shown in Fig. 3(c), a converter rated for a fraction of the dc line voltage builds up the injection current in several cycles by switching a precharged capacitor into the resonant circuit with alternating polarity. The successive oscillation technique requires an external power supply rated for a fraction of the dc line voltage to energize the converter. In contrast to the other injection circuit topologies, the successive oscillation technology inherently adapts to the fault current level without added complexity. This is a clear advantage of the successive oscillation technique because, unlike the other injection circuit topologies, it does not suffer from arc reignitions

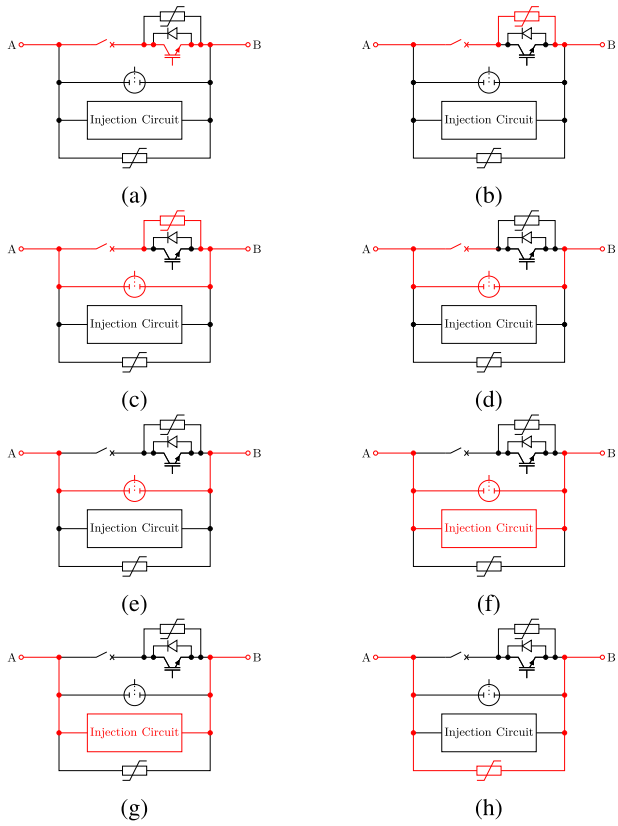

Fig. 4. States of the simplified unidirectional EAR DCCB configuration using *LCS-assisted triggering* during interruption.

when interrupting lower than peak fault current. Therefore, the successive oscillation technique allows a promising design with a smaller and cheaper resonant circuit. Nonetheless, the diode in the commutation path of the originally proposed EAR DCCB configuration would block the injection current in reverse direction. Hence, the successive oscillation technique is incompatible with the originally proposed EAR DCCB configuration.

D. LCS-Assisted Triggering

The minimum voltage requirement and the incompatibility with the successive oscillation technique are disadvantages of the originally proposed EAR DCCB configuration. Both disadvantages are partly due to the diode D and the RC circuit. Hence, an EAR DCCB without diode D and without RC circuit, as shown in Fig. 1(b), would be preferable. For such a configuration to work, the minimum voltage of the DCS must be created internally within the commutation loop formed by the main path and the commutation path. The operation states of this simplified EAR DCCB are illustrated in Fig. 4 exemplary for a unidirectional configuration. Under normal operating conditions, the main path conducts i_{DC} [see Fig. 4(a)]. The EAR DCCB is activated before it is tripped by the dc system protection and it proactively commutates, as described in [28], for the originally proposed EAR DCCB configuration. For proactive commutation, the controller of the EAR DCCB has to sense abnormal operating conditions with, for instance, an overcurrent

criterion. When proactive commutation is initiated, the LCS in the main path is turned OFF to commutate i_{DC} into its snubber circuit [see Fig. 4(b)]. The snubber circuit can be an MOV as depicted or an elaborated design as needed if S is implemented with an ultrafast disconnector instead of an arcing mechanical switch [30]. The snubber circuit absorbs the turn-OFF voltage of the LCS. Since S is still closed, the turn-OFF voltage also appears across the DCS. The DCS is triggered when the turn-OFF voltage surpasses its minimum voltage [see Fig. 4(c)]. Within microseconds, i_{DC} commutates from the snubber circuit to the DCS [see Fig. 4(d)]. The turn-OFF voltage of the LCS does not affect i_{DC} during the fast commutation process because the turn-OFF voltage of the LCS is considerably lower than the voltage rating of the MOV in the energy absorption path. Considering the role of the LCS, this commutation process is referred to as *LCS-assisted triggering*.

Next, S opens while the DCS conducts i_{DC} [see Fig. 4(e)]. This takes several milliseconds depending on the actuator of S. If the dc grid condition is deemed to be noncritical, the EAR DCCB aborts proactive commutation after a set duration. However, if the EAR DCCB receives a trip signal from the dc grid protection or if i_{DC} exceeds the maximum DCCB current, the EAR DCCB starts the interruption process by activating the injection circuit [see Fig. 4(f)]. The injection circuit creates a current zero crossing in the DCS to extinguish the discharge. After that, i_{DC} commutates to the injection circuit to recharge its capacitive storage [see Fig. 4(g)]. The voltage across the injection circuit increases until the MOV in the energy absorption path becomes conductive commutating i_{DC} to the MOV [see Fig. 4(h)]. The MOV imposes a counter voltage, which decreases i_{DC} to zero finishing the interruption process. When the EAR DCCB has cleared the fault, it prepares for reclosing by replenishing the energy storage of the injection circuit and of the actuator for S. In fast auto-reclosing strategies for dc systems with overhead lines, the maximum charge capability and the maximum operating frequency of the DCS have to be obeyed. Common auto-reclosing times like 100 to 300 ms, are not a problem.

In the simplified EAR DCCB configuration, no component is added compared to the originally proposed EAR DCCB configuration and the RC circuit and the diode D are removed. It has to be kept in mind that R_{DCS}, C_{DCS}, and D have to be rated for the DCCB voltage, the voltage imposed by the MOV during interruption, which has to exceed the dc line voltage. Assuming a DCCB voltage by a factor 1.5 higher than the dc line voltage and 5.5 kV diodes, the diode count is reduced by at least 11 for a 40 kV MVDC system and by 88 for a 320 kV HVdc system. Additional voltage balancing circuits for the series connections in the diode valve are not needed either. Overall, the component count is reduced substantially without any tradeoff. The connection to ground within the RC circuit of the originally proposed EAR DCCB is also undesirable in a high voltage design since it introduces stringent and costly isolation requirements. The simplified EAR DCCB configuration is, thus, more cost-effective than the originally proposed EAR DCCB configuration.

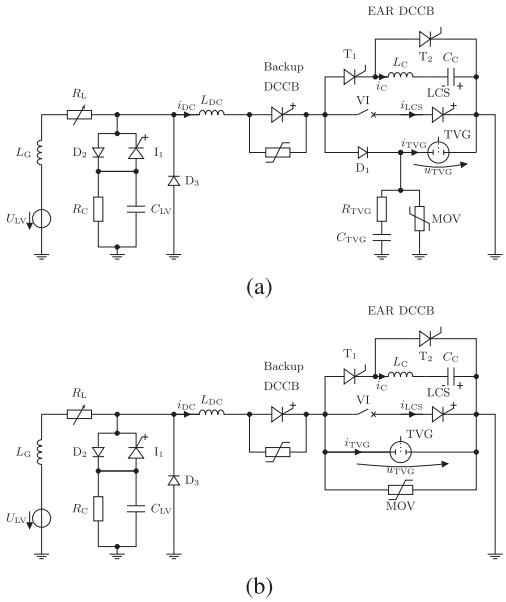

Fig. 5. Advanced test circuit for EAR DCCBs. (a) Originally proposed configuration. (b) Simplified configuration.

III. Test Methodology

A. Advanced Test Circuit

A specialized test circuit, as described in [31] and shown in Fig. 5, is needed to test all functionalities of a DCCB. This test circuit allows to replicate various scenarios, such as auto-reclosing and proactive commutation with combinations of constant load current, fault current, and temporary current. Moreover, the test circuit also includes a backup solid-state DCCB to protect the EAR DCCB if it fails to interrupt or if the DCS conducts for an excessive duration.

B. Experimental Setup

The originally proposed EAR DCCB and the simplified EAR DCCB are tested with the configurations shown in Fig. 5(a) and (b), respectively. A triggered vacuum gap (TVG) is used as DCS and a vacuum interrupter (VI) with a Thomson-coil actuator, described in [29], is used as S in the prototype EAR DCCB. The injection circuit shown in Fig. 3(b) is used because this topology without external power supply simplifies the experimental setup. In this prototype, the protective voltage level of the MOV in the energy absorption path is lower than the rated voltage of the LCS. Therefore, it is sufficient to use a single MOV as snubber of the LCS and for energy absorption. The controller of the prototype is realized in the field programmable gate array part of a Xilinx system-on-a-chip on the ZedBoard. The controller has an input from the protection system for the external trip signal and an auto-reclosing enable flag. The controller also has an interface to the controller of the VI system via optical fibres. The Hall-effect-based current sensors LEM HAT 800-S are used to measure the total DCCB current and the current in the TVG for the controller. Depending on the DCCB current level, the controller activates

TABLE I
PARAMETERS OF DCCB TEST CIRCUIT AND EAR DCCB

I_L/A	I_F/A	U_{LV}/kV	U_{TVG}/kV	L_{DC}/mH	C_{LV}/mF	R_C/kΩ	R_L/Ω	R_{TVG}/Ω	C_{TVG}/μF	L_C/μH	C_C/μF
150	1200	0.5	2.8	1.4	11.2	10	3.3	1-15	10	9	60

proactive commutation. Apart from that the current measurements are currently only used for internal DCCB protection against overcurrent and excessively long conduction of the TVG. The test settings, DCCB settings, and the triggering delay of the TVG are set via a software interface. In an industrial application, aging could affect the interaction between LCS and TVG during LCS-assisted triggering. Therefore, the voltage across the TVG should be directly or indirectly measured, for instance in the gate driver of the LCS, in the simplified configuration to adjust the triggering delay of the TVG correspondingly. The parameters of the prototype and test circuit are given in Table I with the maximum constant dc I_L and peak fault current I_F.

The experimental setup, shown in Fig. 6, is based on a prototype from a previous Ph.D. project [32]. The IGCT power supply, the triggering unit of the TVG, and the resonant circuit of the injection circuit are mounted below the base plate of the EAR DCCBs and, hence, cannot be seen in Fig. 6. For safety reasons, the experimental setup is housed in an explosion-proof test room and the experimental setup is automated.

C. Test Procedures

Tests involving the VI are complex, although the VI itself has a limited impact on the experimental results. The VI is usually operated without arcing similar to a disconnector and, consequently, does not affect the internal commutation processes of the EAR DCCB. Thus, the VI is left unconnected in the tests, in which the VI is not the subject of interest, to reduce the complexity. A diode is inserted instead of the VI since the injection current would otherwise freewheel through the intrinsic antiparallel diode of the IGCT used as LCS. The following tests of aspects fundamental to the successful operation of EAR DCCBs are executed.

1) Triggering of TVG: The triggering characteristics of the TVG are studied using the configuration shown in Fig. 5(a), particularly focusing on the minimum voltage. According to the manufacturer of the TVG, the theoretical minimum voltage is 15 to 20 V. However, it is recommended not to operate below 50 V to avoid damaging the TVG. First, the RC circuit is precharged by turning ON and OFF the backup DCCB. Second, the TVG is triggered manually. R_{DCS} is varied to analyze the effect of the current provided by the RC circuit and of the RC time constant on the triggering process.

2) Commutation from main path to commutation path: Commutation from the main path to the commutation path can only succeed if the TVG is triggered successfully. The commutation process is affected by the delay between triggering the TVG and turning OFF the LCS and possible interactions of the discharge in the TVG with the RC circuit, among other factors. The diode replacing the VI as described previously can introduce phenomena not representative for EAR DCCBs since the parasitic elements

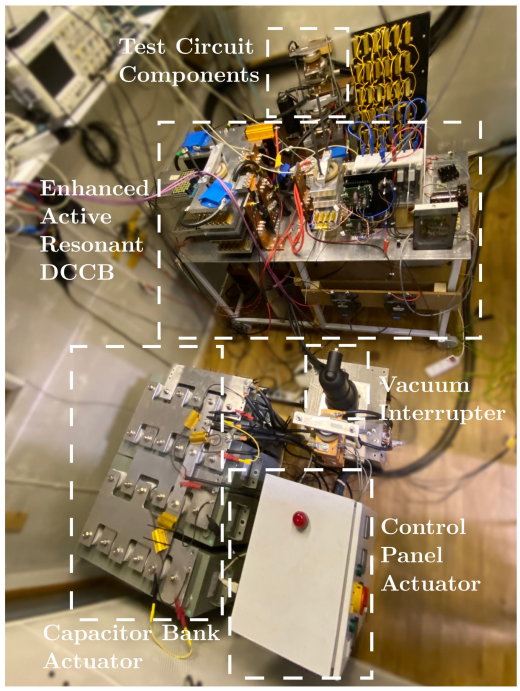

(a)

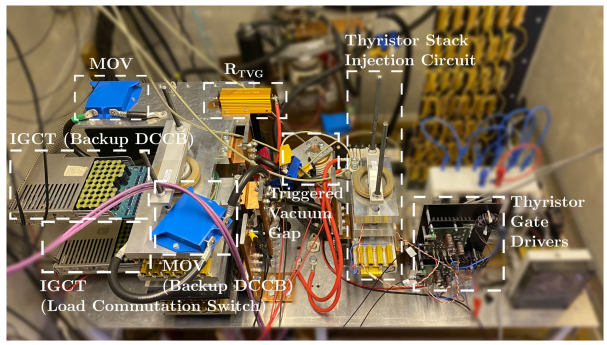

(b)

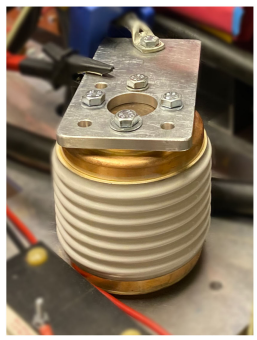

(c)

Fig. 6. Experimental setup used to test the EAR DCCB. (a) Overview of the experimental setup. (b) Enhanced active resonant DC circuit breaker prototype. (c) Close-up of the triggered vacuum gap.

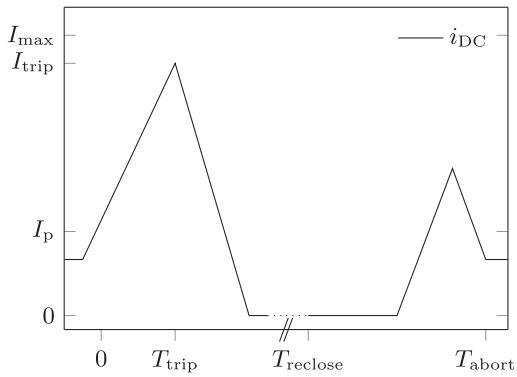

Fig. 7. Test scenario to study the capability of EAR DCCBs to abort proactive commutation.

of the diode and its dynamical properties can lead to interactions with the discharge in the TVG. Therefore, the diode is shorted in this test. A temporary fault with a defined peak current is used as test scenario because it does not require the EAR DCCB to interrupt. Hence, the injection circuit is not activated at all and freewheeling of the injection current through the antiparallel diode of the LCS is avoided. The commutation process takes a few microseconds and the test current is practically constant during this time.

3) Auto-reclosing: Auto-reclosing can be executed with the main path, the VI, or with the commutation path, the TVG. However, the triggering unit of the TVG used is only capable of operating the TVG at 1 Hz, which is substantially slower than typical deionization times of arc faults. Consequently, reclosing is attempted after 1.107 s (experimentally determined to work) in the commutation path reclosing tests.

4) Memory effect: Using proactive commutation also requires the capability to abort this operation state again. This is done by reclosing the VI and then turning ON the LCS. The discharge voltage of the TVG is higher than the voltage drop across the main path, thus commutating i_{DC} from the TVG back to the main path. The abortion of proactive commutation was demonstrated in [28]. However, in one of the very first experiments immediately after an interruption test, proactive commutation could not be aborted. Hypothetically, the relatively high current of the interruption test could have altered the initial state of the TVG in its next operation. To exclude a potentially detrimental memory effect, the abortion of proactive commutation has to be studied systematically. The test scenario used, as illustrated in Fig. 7, starts with load current followed by a fault with subsequent auto-reclosing followed by a temporary fault and ends with the load current. The EAR DCCB should be able to abort proactive commutation at the end of the test scenario. Tests are run every 20 min to assure that the TVG is in the same state in each test.

IV. Experimental Results

A. Triggering of TVG

Fig. 8 studies the triggering of the TVG with different precharge voltages and $R_{\text{TVG}} = 4.7\,\Omega$. Initially, the voltage

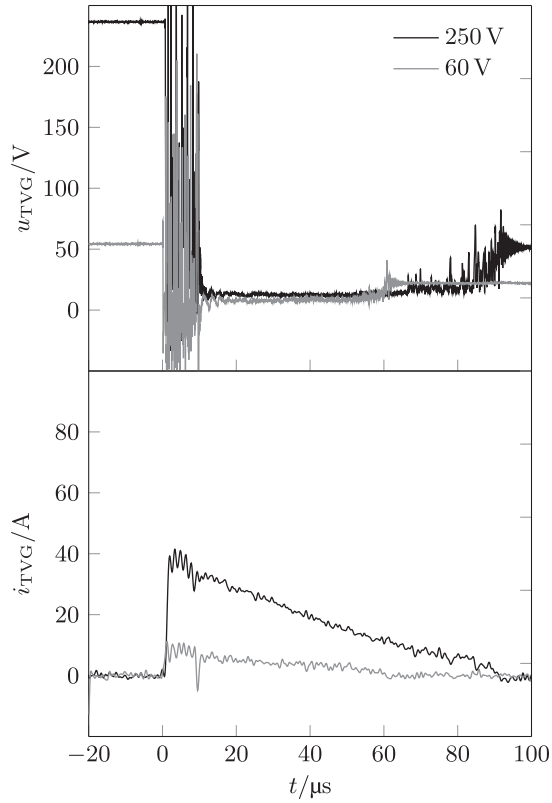

Fig. 8. Triggering tests of the TVG for various RC circuit precharge voltages with $R_{\text{TVG}} = 4.7\,\Omega$.

across the TVG u_{TVG} equals the voltage across C_{TVG}. The forming phase immediately after triggering is characterized by high-frequency discharge voltage oscillations with peaks of several kilovolts while the discharge is forming in the TVG. When the discharge burns in the conduction phase, the discharge voltage and forming current are less volatile compared with the forming phase. C_{TVG} discharges into the TVG until the voltage across the RC circuit decreases below the minimum voltage necessary to sustain the discharge. At the end of the conduction phase, the discharge voltage and i_{TVG} begin to fluctuate again and the discharge in the TVG extinguishes. After that, u_{TVG} equals the residual voltage of C_{TVG}. The observed waveforms do not change qualitatively for the voltage levels tested since the current provided by the RC circuit is relatively low. Nevertheless, the discharge voltage tends to be more chaotic for decreasing current.

Fig. 9 shows the discharge voltage during the conduction phase and extinction phase for various R_{TVG} at a pre-charge voltage of 60 V. During the conduction phase, R_{TVG} barely affects the discharge voltage. However, the discharge extinguishes earlier with a larger residual voltage across C_{TVG} for increasing R_{TVG} because the lower current is chopped OFF earlier and the RC circuit does not completely discharge.

The discharge in the TVG is highly stochastic, as shown in Fig. 10, for several measurements with $R_{\text{TVG}} = 1\,\Omega$ and $R_{\text{TVG}} = 15\,\Omega$. Even in this low-current regime, the discharge voltage is remarkably more volatile with strong oscillations for higher R_{TVG}, because of the lower forming current. The

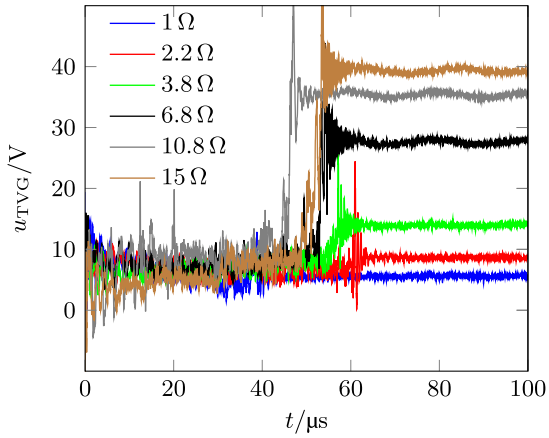

Fig. 9. Triggering tests of the TVG with an RC circuit precharge voltage of 60 V and various R_{TVG}.

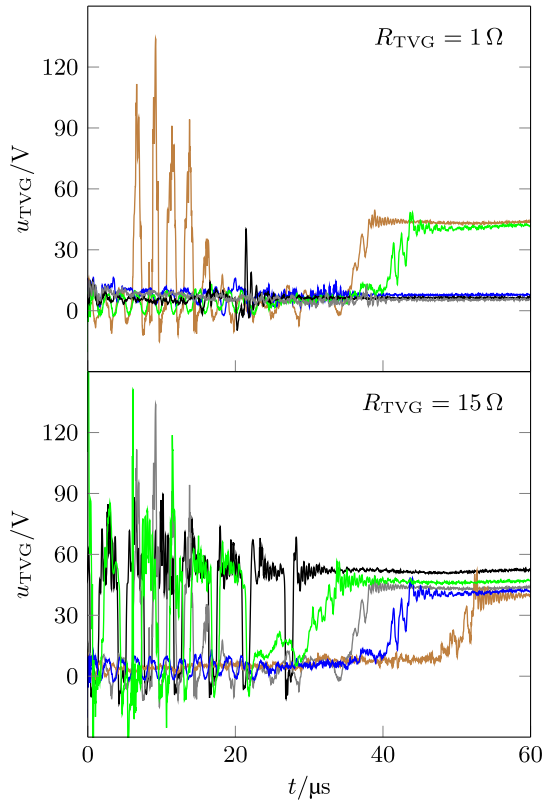

Fig. 10. Triggering tests of the TVG at 60 V.

discharge voltage oscillations also affect the discharging of the RC circuit and can lead to premature discharge extinction as evident by the higher residual voltage across C_{TVG}. Despite the highly volatile discharge voltage, the TVG triggers reliably and mistriggering has not been observed in the experiments. Nonetheless, the TVG will not trigger any more if R_{TVG} is increased further. The forming current would be too small to sustain the discharge and the capacitor energy would dissipate in the discharge without proper commutation.

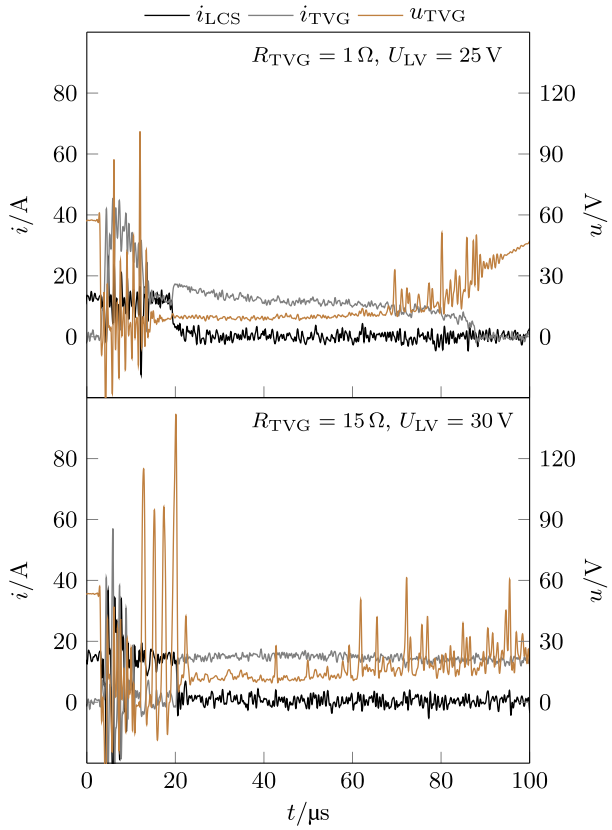

Fig. 11. Commutation from the load commutation switch to the TVG of the originally proposed EAR DCCB configuration.

B. Commutaton From Main Path to TVG

1) Originally Proposed Commutation: The internal DCCB currents and u_{TVG} during the commutation from the main path to the commutation path of the originally proposed EAR DCCB configuration are shown in Fig. 11 at a relatively low current. For $R_{\mathrm{TVG}} = 1\,\Omega$, the commutation succeeds at $t = 19\,\mu\mathrm{s}$. Then, the discharge in the TVG becomes unstable and the discharge voltage fluctuates until the current in the TVG is interrupted at $t = 87.4\,\mu\mathrm{s}$. For $R_{\mathrm{TVG}} = 15\,\Omega$, the discharge voltage is also volatile, but the discharge does not extinguish. Despite the stochastic nature of the discharge, the outcomes for commutation were consistent in the experiments. Nevertheless, the discharge in the TVG did occasionally not extinguish after commutation for $R_{\mathrm{TVG}} = 1\,\Omega$.

At increased voltage and current, commutation with $R_{\mathrm{TVG}} = 1\,\Omega$ does not fail, as shown in Fig. 12, since the volatility of the discharge voltage reduces with increasing current.

A closeup of the commutation process is shown in Fig. 13. For $R_{\mathrm{TVG}} = 1\,\Omega$, the current in the TVG equals the forming current from the RC circuit prior to the commutation. The current in the TVG collapses at $t = 12\,\mu\mathrm{s}$ with tremendous positive discharge voltage peaks. This indicates a discharge instability, which could be due to physical phenomena in the discharge or interactions with the RC circuit. Commutation is also tested with various delays between the triggering of the TVG and the turn-OFF of the LCS. Obviously, the delay cannot be arbitrarily large because

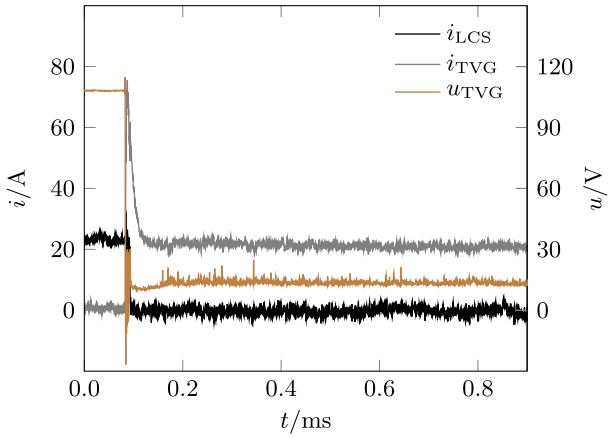

Fig. 12. Commutation from the load commutation switch to the TVG of the originally proposed EAR DCCB configuration with $R_{\mathrm{TVG}} = 1\,\Omega$ at $U_{\mathrm{LV}} = 50\,\mathrm{V}$.

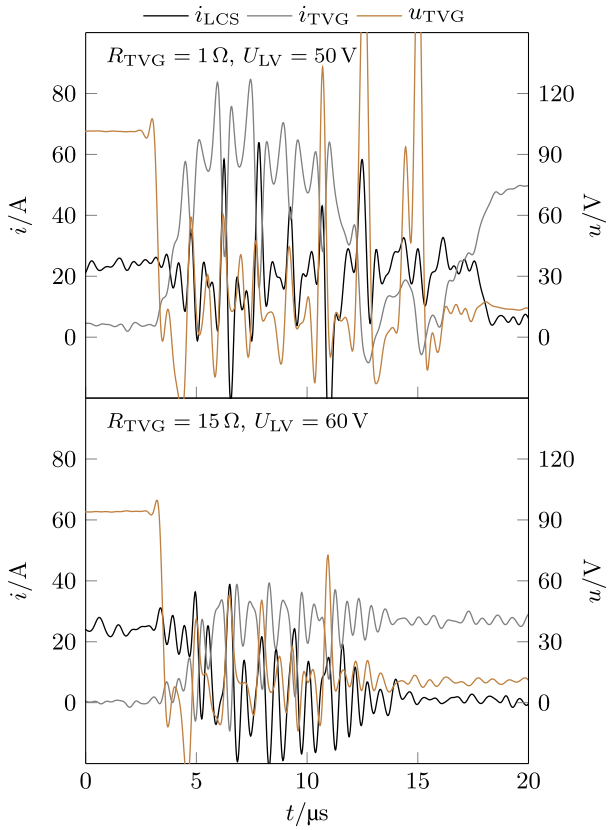

Fig. 13. Closeup of commutation from the load commutation switch to the TVG of the originally proposed EAR DCCB configuration.

the discharge in the TVG would extinguish at a current close to zero before the commutation. Apart from that, the delay is irrelevant for the success of the commutation process, which can even succeed during the forming phase of the discharge, as depicted in Fig. 13, for $R_{\mathrm{TVG}} = 15\,\Omega$. The commutation process is, however, slower in the forming phase compared with the conduction phase.

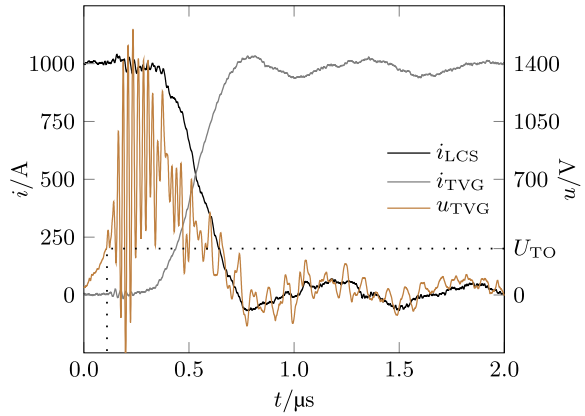

Fig. 14. Closeup of the commutation from the load commutation switch to the TVG of the simplified EAR DCCB configuration with LCS-assisted triggering and t_{TVG}=1.417 μs.

2) LCS-Assisted Triggering: A closeup of the commutation process in the simplified EAR DCCB configuration with LCS-assisted triggering is shown in Fig. 14. With the chosen triggering delay t_{TVG} between the turn-OFF of the LCS and the triggering of the TVG, the TVG is triggered when the turn-OFF voltage of the LCS U_{TO} is approximately 280 V and the commutation succeeds within 1 μs. Immediately after triggering, discharge voltage oscillations comparable to the originally proposed commutation process are visible. The volatility of the discharge voltage is actually reduced with LCS-assisted triggering and commutation did not fail once at any of the current levels tested from 10 to 1200 A. Thus, the stochastic nature of the discharge in the TVG does not affect LCS-assisted triggering.

The triggering delay is critical for LCS-assisted commutation because it has to be chosen to assure that U_{TO} exceeds the minimum voltage of the TVG. By careful selection of the triggering delay, LCS-assisted triggering works at any current level. Fig. 15(a) shows how the triggering delay affects U_{TO}. The triggering delay has to be adapted for each current level to limit the turn-OFF voltage of the LCS since the turn-OFF voltage of the LCS increases faster with increasing current, as shown in Fig. 15(b).

C. Interruption

The interruption capability of originally proposed EAR DCCB configuration was already studied in [28]. The results from interruption tests of the simplified EAR DCCB configuration in Fig. 5(b) with LCS-assisted triggering are shown in Fig. 16 up to 1200 A. In these tests, the VI is connected to resemble operation in industrial applications, even though the VI does not influence the commutation processes as described before. The simplified EAR DCCB configuration works as expected in the tests, which demonstrates its feasibility.

D. Auto-Reclosing

1) Memory Effect: The potential memory effect is studied with the originally proposed and simplified EAR DCCB configuration and the test scenario shown in Fig. 7. The peak

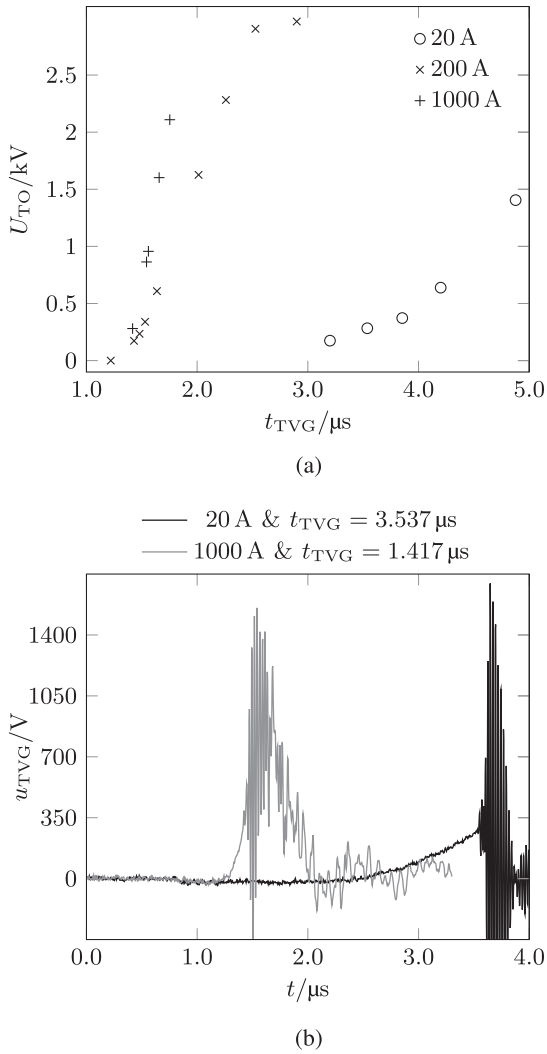

Fig. 15. Study of the turn-OFF voltage for *LCS-assisted triggering*. (a) Discharge voltage of the triggered vacuum gap at triggering instance for various triggering delays at various current levels. (b) Discharge voltage of the triggered vacuum gap starting at turn-OFF of the load commutation switch.

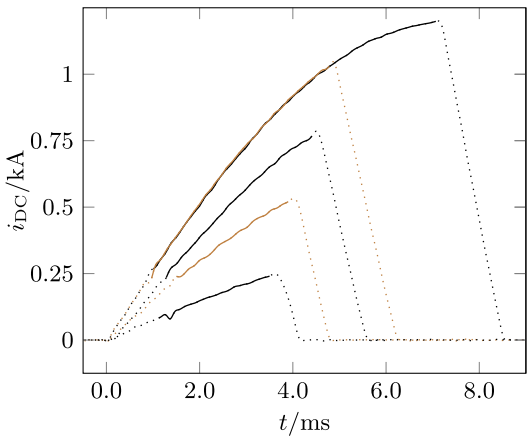

Fig. 16. DC interruption tests of the simplified EAR DCCB configuration with *LCS-assisted triggering*. The solid part of the traces corresponds to the state shown in Fig. 4(e), in which the TVG conducts i_{DC}.

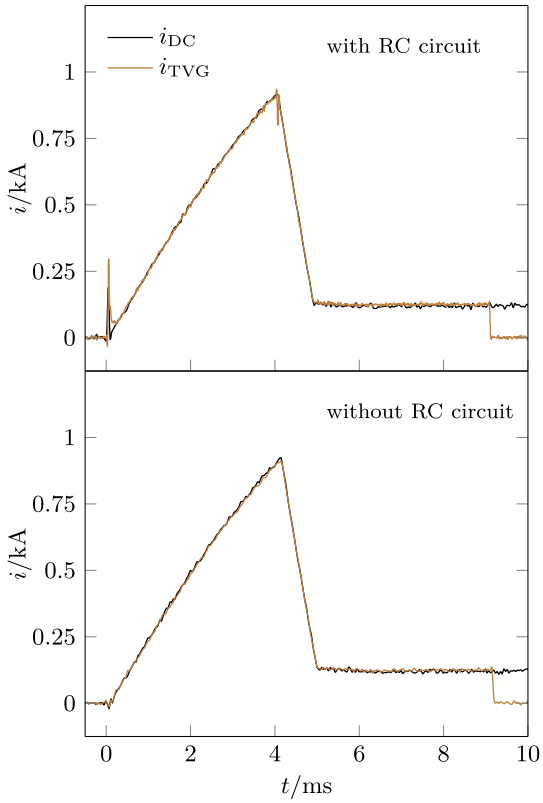

Fig. 17. Temporary fault after auto-reclosing operation of the EAR DCCB with the TVG and subsequent commutation to the main path.

fault current is set to 1000 A and the peak temporary fault is set between 300 to 900 A. Reclosing is executed with the TVG and only this part of the experiment is shown in Fig. 17. LCS-assisted triggering is not used for auto-reclosing with the simplified EAR DCCB configuration since the dc-line voltage provides the voltage required by the TVG in this case. The only difference between both configurations is that the RC circuit provides an initial current for the TVG in the originally proposed configuration, which is visible at $t = 0$ in the upper graph. Both configurations succeed to reclose with the TVG and to commutate i_{DC} from the TVG back to the main path after i_{DC} decayed. This result is reproduced for all temporary fault current tested and, thus, the memory effect does not exist. The unsuccessful abortion of proactive commutation after an interruption test described in Section III-C4 was a singular event due to another cause. For instance, improper conditioning of the TVG prior to the first experiments could have affected the discharge in the DCS adversely. Given the above-mentioned, EAR DCCBs feature proactive commutation because they can reliably abort this operation state.

2) Commutation Path Reclosing: Fig. 18 shows a scenario in which the originally proposed and simplified EAR DCCB configuration interrupt a fault current, reclose with the TVG, and then clear the persisting fault in a second interruption. As visible, the EAR DCCB does not need to commutate i_{DC} from the TVG back to the main path after reclosing and can instead interrupt the fault current directly with current injection. The EAR DCCBs could also clear the persisting fault without delay since the VI

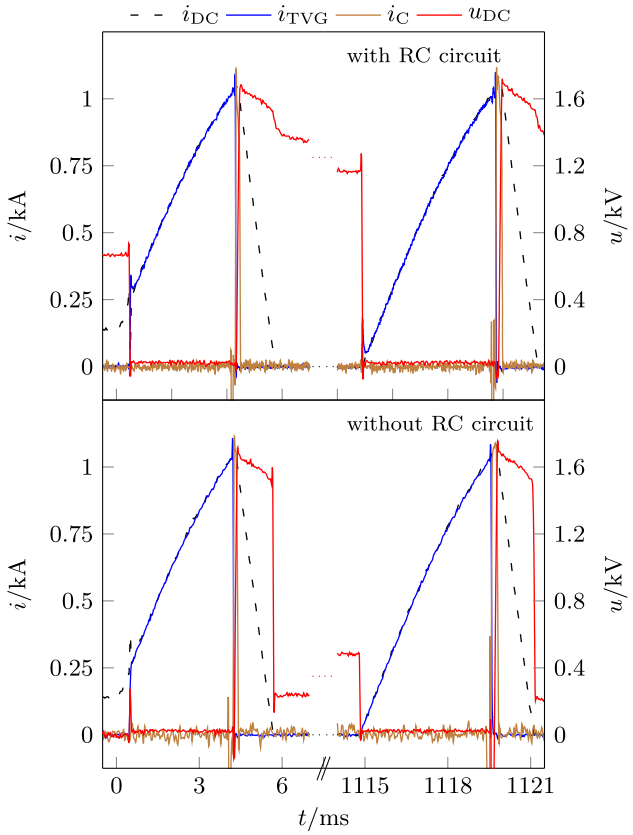

Fig. 18. Auto-reclosing operation of the EAR DCCB with the TVG and persisting fault.

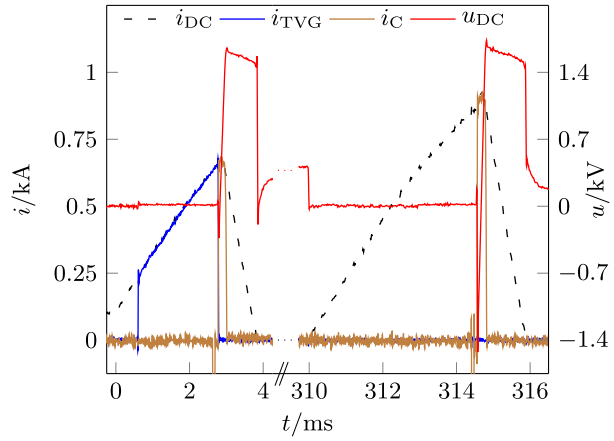

Fig. 19. Auto-reclosing operation of the simplified EAR DCCB configuration with the VI.

is not operated. However, the capacitor of the injection circuit is recharged to a higher voltage during the first interruption, which would entail a too large injection current for an earlier second interruption at lower current. Therefore, the current trip level after reclosing is implemented to be equal to the regular current trip level. The reclosing operation works similarly for the originally proposed and simplified EAR DCCB configuration. The reason for the difference in u_{TVG} for both configuration is that the MOV is connected differently.

3) Main Path Reclosing: Auto-reclosing operation of the simplified EAR DCCB with the VI is demonstrated in Fig. 19. Auto-reclosing is initiated 300 ms after the first dc interruption by reclosing the VI and the fault current immediately rises again. The triggering unit of the TVG is not ready yet and hence, proactive commutation is not possible. When the trip current is surpassed, the VI is opened with an arc. In the second interruption, current injection extinguishes the arc in the VI. The peak current is higher compared with the previous dc interruption because the protection delay cannot be compensated with proactive commutation.

V. Discussion

The expected volatile nature of the discharge in the TVG at low current and high-frequency oscillations, especially in the forming phase, do not adversely affect the operation of EAR DCCBs. It would, nonetheless, be interesting to know more about the discharge processes in the TVG. Vacuum arcs and the role of the cathode spots have been extensively researched in the past. Vacuum arcs mainly burn in a diffuse regime and a constricted regime. The vacuum arc voltage is oscillatory in the diffuse regime and relatively stable in the constricted regime. Apart from the stochastic oscillations observed, the discharge voltage was relatively stable around 10 to 15 V, which indicates that the discharge in the TVG is an arc discharge. Considering the low current used in these experiments, the vacuum arc is most probably in the diffuse regime. The behavior of vacuum arcs in VIs at low current was already studied in [33]. Even though similarities to VIs are likely, the cause of the substantial discharge voltage oscillations in the conduction phase of the TVG at low current has yet to be understood. Possibly, the discharge in the interelectrode gap is never fully established during the oscillations in the forming phase and conduction phase, and the current in the device is maintained by the forming glow discharge between cathode and triggering electrode. The high positive voltage excursions could be indicative for a cathode spot trying not to extinct at low current. Theoretically, the discharge could also oscillate back and forth between the triggering electrode and the cathode after triggering with current inflow from the anode. Interactions of the discharge with the RC circuit of the originally proposed EAR DCCB configuration should be considered because the voltage oscillations did not occur in the experiments with the simplified EAR DCCB configuration. Nonetheless, the experimental results show that the minimum voltage requirement of approximately 50 V and low current operation down to 50 A are not a severe limitation for the originally proposed EAR DCCB configuration.

The failed commutations to the commutation path of the originally proposed EAR DCCB configuration at low R_{TVG} shows that the choice of R_{TVG} has a lower bound. R_{TVG} has a higher bound as well since the TVG does not trigger at all if R_{TVG} limits the forming current below a certain level. The fault impedance adds to the impedance of the RC circuit during the triggering phase, which has to be considered for the upper bound of R_{TVG}. It is, therefore, relatively complex to dimension the RC circuit such that the originally proposed

EAR DCCB configuration can operate at a wide range of fault impedances. Thus, the inherent redundancy of the originally proposed EAR DCCB configuration using mechanical switches instead of disconnectors, described in [28], is indispensable for reliable interruption.

As demonstrated, auto-reclosing can be executed with either the main path, the VI, or the commutation path, the TVG. However, several commutation path auto-reclosing tests without persisting fault exhibited commutation failure after successful triggering, which still requires research for clarification. As for now, it is unclear whether these problems are technology or implementation related. In the experiments with the originally proposed EAR DCCB configuration, the problem occurred only for $R_{\mathrm{TVG}} = 1\,\Omega$ and not with $R_{\mathrm{TVG}} = 4.7\,\Omega$ and $R_{\mathrm{TVG}} = 15\,\Omega$. The simplified EAR DCCB configuration inconsistently exhibited this problem with and without persisting fault. Connecting an RC snubber dimensioned as the RC circuit of the originally proposed EAR DCCB configuration in parallel to the TVG of the simplified EAR DCCB configuration improved commutation reliability, however, not to an acceptable level. Another disadvantage of commutation path auto-reclosing is that the TVG potentially cannot be immediately triggered again after the subsequent commutation to the main path. Hence, a mechanical switch would be required instead of a UFD to handle persisting faults.

Overall, the simplified EAR DCCB configuration reduces the component count considerably and allows for a more cost-effective design than the originally proposed EAR DCCB configuration. LCS-assisted triggering improves the operational reliability because the commutation process is decoupled from the dc grid and its influence on the voltage potential at the cathode of the DCS. Moreover, the simplified EAR DCCB configuration can be combined with any injection circuit implementation because the current in the commutation path is not rectified. Symmetric bidirectionality can be implemented in a simpler way as compared with the originally proposed EAR DCCB configuration by anti-parallelly connecting DCSs. The simpler structure of the commutation path of the simplified EAR DCCB configuration allows for a modularized design similar to hybrid DCCBs facilitating features, such as fault current limitation. The modularization also eases the design of EAR DCCBs for HVdc. For instance, each module could be implemented with a 55 kV TVG with a total of six modules for a 320-kV HVdc system. Therefore, it is recommended to adopt the simplified EAR DCCB configuration for HVdc. For industrial applications, the EAR DCCB can be built with already available components, such as VIs, TVGs, and IGBTs. For MVdc, the EAR DCCB design would resemble common ac metal-enclosed switchgear and does not require any modularization since VIs and TVGs with suitable ratings are available. For HVdc, the EAR DCCB design would have a physical layout similar to the DCCBs from [11] and [7]. Even though MVdc and HVdc designs would differ from the prototype studied, it is expected that the findings of this study are equally valid because the underlying operating mechanisms do not change.

For future research, it would be interesting to investigate the possibility to integrate the DCS as auxiliary contact gap in the mechanical switch. The arc in the mechanical switch could provide charge carriers that reduce the triggering requirements of the auxiliary contact gap. In certain applications, it may be preferable not to use an LCS, for instance, because of the losses, and LCS-assisted triggering cannot be applied. Instead, a fast mechanical switch could build up an arc voltage sufficient to commutate i_{DC} from the main path to the commutation path [34]. In this case, the originally proposed EAR DCCB configuration could potentially commutate faster compared with the simplified EAR DCCB configuration.

VI. Conclusion

This article studied the originally proposed EAR DCCBs and the simplified EAR DCCBs that use LCS-assisted commutation experimentally. The experiments showed that the DCS used, the TVG, triggers reliably down to 50 V and at current as low as 20 A despite substantial discharge voltage oscillations. Thus, the minimum voltage requirement of the DCS is not as critical as previously expected. However, the RC circuit of the originally proposed EAR DCCB configuration must be carefully tuned for reliable commutation from the main path to the commutation path at low current. For LCS-assisted commutation to work reliably, the triggering delay must be adapted depending on the current level. Moreover, proactive commutation operation, main path auto-reclosing, and commutation path auto-reclosing were demonstrated. If an LCS is used in the EAR DCCB configuration, LCS-assisted triggering allows to simplify the EAR DCCB configuration, to reduce the component count, and to improve commutation reliability under all operating conditions. Hence, the simplified EAR configuration is superior to the originally proposed EAR DCCB configuration in most applications.

References

[1] D. Jovcic, G. Tang, and H. Pang, "Adopting circuit breakers for high-voltage DC networks: Appropriating the vast advantages of DC transmission grids," *IEEE Power Energy Mag.*, vol. 17, no. 3, pp. 82–93, May/Jun. 2019.

[2] M. Barnes, D. S. Vilchis-Rodriguez, X. Pei, R. Shuttleworth, O. Cwikowski, and A. C. Smith, "HVDC circuit breakers a review," *IEEE Access*, vol. 8, pp. 211829–211848, 2020.

[3] Y. Wang and R. Marquardt, "Performance of a new fast switching DC-Breaker for meshed HVDC-grids," in *Proc. 17th Eur. Conf. Power Electron. Appl.*, 2015, pp. 1–9.

[4] B. C. Kim, Y. H. Chung, H. D. Hwang, and H. S. Mok, "Comparison of inverse current injecting HVDC curcuit breaker," in *Proc. 3rd Int. Conf. Elect. Power Equip. - Switching Technol.*, 2015, pp. 501–505.

[5] T. Heinz, P. Hock, and V. Hinrichsen, "Comparison of artificial current zero impulses for a vacuum interrupter based direct current circuit breaker," in *Proc. 27th Int. Symp. Discharges Elect. Insul. Vacuum*, 2016, pp. 1–4.

[6] K. Tahata *et al.*, "HVDC circuit breakers for HVDC grid applications," in *Proc. 11th IET Int. Conf. AC DC Power Transmiss.*, 2015, pp. 1–9.

[7] L. Ängquist, S. Norrga, T. Modeer, and S. Nee, "Fast HVDC breaker using reduced-rating power electronics," in *Proc. 13th IET Int. Conf. AC DC Power Transmiss.*, 2017, pp. 1–6.

[8] A. Jehle and J. Biela, "Hybrid circuit breaker for HVDC grids with controllable pulse current shape," in *Proc. 19th Eur. Conf. Power Electron. Appl.*, 2017, pp. 1–10.

[9] M. Pathmanathan, G. Zanuso, Z. Zhang, S. Valdemarsson, and E. Johansson, "Self-powered supply and control system for hybrid semiconductor DC switch," in *Proc. 20th Eur. Conf. Power Electron. Appl.*, 2018, pp. 1–10.

[10] R. Sander, M. Suriyah, and T. Leibfried, "Characterization of a countercurrent injection-based HVDC circuit breaker," *IEEE Trans. Power Electron.*, vol. 33, no. 4, pp. 2948–2956, Apr. 2018.

[11] J. Häfner and B. Jacobson, "Proactive hybrid HVDC breakers—A key innovation for reliable HVDC grids," in *Proc. CIGRÉ Symp.*, 2011, pp. 1–8.
[12] C. Davidson, R. Whitehouse, C. Barker, J.-P. Dupraz, and W. Grieshaber, "A new ultra-fast HVDC circuit breaker for meshed DC networks," in *Proc. 11th IET Int. Conf. AC DC Power Transmiss.*, 2015, pp. 1–7.
[13] W. Zhou *et al.*, "Development and test of a 200 kV full-bridge based hybrid HVDC breaker," in *Proc. 17th Eur. Conf. Power Electron. Appl.*, 2015, pp. 1–7.
[14] L. Liu, J. Zhuang, C. Wang, Z. Jiang, J. Wu, and B. Chen, "A hybrid DC vacuum circuit breaker for medium voltage: Principle and first measurements," *IEEE Trans. Power Del.*, vol. 30, no. 5, pp. 2096–2101, Oct. 2015.
[15] W. Wen *et al.*, "Research on a current commutation drive circuit for hybrid DC circuit breaker and its optimization design," *IET Gener., Transmiss., Distrib.*, vol. 10, no. 13, pp. 3119–3126, Oct. 2016.
[16] F. Xu *et al.*, "Topology, control and fault analysis of a new type HVDC breaker for HVDC systems," in *Proc. IEEE PES Asia-Pacific Power Energy Eng. Conf.*, 2016, pp. 1959–1964.
[17] G. Liu, F. Xu, Z. Xu, Z. Zhang, and G. Tang, "Assembly HVDC breaker for HVDC grids with modular multilevel converters," *IEEE Trans. Power Electron.*, vol. 32, no. 2, pp. 931–941, Feb. 2017.
[18] L. Feng, R. Gou, X. Yang, F. Zhuo, and S. Shi, "Research on the current commutation in a novel hybrid HVDC circuit breaker," in *Proc. 19th Eur. Conf. Power Electron. Appl.*, 2017, pp. 1–9.
[19] A. Daibo *et al.*, "High-speed current interruption performance of hybrid DCCB for HVDC transmission system," in *Proc. 4th Int. Conf. Elect. Power Equip. - Switching Technol.*, 2017, pp. 329–332.
[20] L. Feng, R. Gou, F. Zhuo, X. Yang, and F. Zhang, "Research on the breaking branch for a hybrid DC circuit breaker in 500 kV voltage-sourced converter high-voltage direct current grid," *IET Power Electron.*, vol. 13, no. 16, pp. 3560–3570, Dec. 2020.
[21] M. K. Bucher and C. M. Franck, "Fault current interruption in multiterminal HVDC networks," *IEEE Trans. Power Del.*, vol. 31, no. 1, pp. 87–95, Feb. 2016.
[22] L. Mackey, C. Peng, and I. Husain, "Progressive switching of hybrid DC circuit breakers for faster fault isolation," in *Proc. IEEE Energy Convers. Congr. Expo.*, 2018, pp. 7150–7157.
[23] H. Gallagher, G. Hofmann, and M. Lutz, "The crossed field switch tube-A new HVDC circuit interrupter," *IEEE Trans. Power App. Syst.*, vol. PAS-92, no. 2, pp. 702–709, Mar. 1973.
[24] C. Davidson, C. Barker, J. De Bedout, W. Grieshaber, J. Bray, and T. Sommerer, "Hybrid DC circuit breakers using gas-discharge tubes for high-voltage switching," in *Proc. CIGRÉ Winnipeg Colloq.*, 2017, pp. A3–B4.
[25] L. Feng, R. Gou, X. Yang, F. Wang, F. Zhuo, and S. Shi, "A 320kv hybrid HVDC circuit breaker based on thyristors forced current zero technique," in *Proc. IEEE Appl. Power Electron. Conf. Expo.*, 2017, pp. 384–390.
[26] W. Pan, F. Zhuo, Y. Chen, X. Du, L. Feng, and S. Shi, "A passive hybrid HVDC circuit breaker based on thyristors," in *Proc. 19th Eur. Conf. Power Electron. Appl.*, 2017, pp. 1–7.
[27] D. Keshavarzi, E. Farjah, and T. Ghanbari, "Hybrid DC circuit breaker and fault current limiter with optional interruption capability," *IEEE Trans. Power Electron.*, vol. 33, no. 3, pp. 2330–2338, Mar. 2018.
[28] T. Augustin, M. Becerra, and H.-P. Nee, "Enhanced active resonant DC circuit breakers based on discharge closing switches," *IEEE Trans. Power Del.*, vol. 36, no. 3, pp. 1735–1743, Jun. 2021.
[29] T. Augustin, M. Parekh, J. Magnusson, M. Becerra, and H.-P. Nee, "Thomson-coil actuator system for enhanced active resonant DC circuit breakers," *IEEE Trans. Emerg. Sel. Topics Power Electron.*, vol. 10 , no. 1, 2021. doi: 10.1109/JESTPE.2021.3083585.
[30] A. Hassanpoor, J. Häfner, and B. Jacobson, "Technical assessment of load commutation switch in hybrid HVDC breaker," *IEEE Trans. Power Electron.*, vol. 30, no. 10, pp. 5393–5400, Oct. 2015.
[31] T. Augustin, M. Becerra, and H.-P. Nee, "Advanced test circuit for DC circuit breakers," in *Proc. 20th Eur. Conf. Power Electron. Appl.*, 2018, pp. 1–8.
[32] M. Heuvelmans, "Cost-effective cells for high-power modular multilevel converters," Ph.D. dissertation, Dept. Electr. Power Energy Syst., KTH Royal Inst. Technol., Stockholm, Sweden, 2018.
[33] R. P. P. Smeets, "Stability of low-current vacuum arcs," *J. Phys. D*, vol. 19, no. 4, pp. 575–587, Apr. 1986.
[34] M. Parekh, J. Magnusson, G. Engdahl, and M. Becerra, "Arc characteristics of ultra-fast opening switching contacts in hybrid breakers," *IEEE Trans. Power Del.*, vol. 36, no. 5, pp. 2872–2880, Oct. 2021.

Tim Augustin was born in Berlin, Germany. He received the Diplom-Ingenieur degree in electrical engineering in 2015 from the Dresden University of Technology, Dresden, Germany. He is currently working toward the Ph.D. degree with the KTH Royal Institute of Technology, Stockholm, Sweden, and conducts research on dc circuit breakers.

His research interests include power electronics, switching devices, and electrical machines.

Marley Becerra (Senior Member, IEEE) was born in Bogotá, Colombia. He received the B.Sc. and M.Sc. degrees in electrical engineering from the National University of Colombia, Bogot, Colombia, in 2000 and 2003, respectively, and the Phil. Lic. and Ph.D. degrees from Uppsala University, Uppsala, Sweden, in 2006 and 2008, respectively.

He joined ABB Corporate Research, Västerås, Sweden, in 2008, as a Scientist working in the area of power switching technologies. In 2010, he also joined the School of Electrical Engineering, KTH Royal Institute of Technology, Stockholm, as an Assistant Professor in the area of smart grid power components. Since then, he is sharing his time between industry (ABB) as a Principal Scientist and academia (KTH) as an Associate Professor. He has authored or coauthored more than 80 scientific papers in journals and international conferences. His research interests include lightning physics, electrical discharges in gases and liquids, plasma-material interaction, multiphysics modeling, and applied physics in electrotechnologies.

Hans-Peter Nee (Fellow, IEEE) was born in Västerås, Sweden, in 1963. He received the M.Sc., Licenciate, and Ph.D. degrees from the KTH Royal Institute of Technology, Stockholm, Sweden, in 1987, 1992, and 1996, respectively, all in electrical engineering.

Since 1999, he has been a Professor of power electronics with the Department of Electrical Engineering, KTH Royal Institute of Technology. His research interests include power electronic converters, semiconductor components, and control aspects of utility applications, such as FACTS and high-voltage direct-current transmission, and variable-speed drives.

Dr. Nee was a member of the Board of the IEEE Sweden Section for many years and was the Chair of the Board from 2002 to 2003. He is also a member of the European Power Electronics and Drives Association and is involved with its Executive Council and International Steering Committee.